NJC

View Online
Dynamic Article Links

Cite this: *New J. Chem.*, 2011, **35**, 2258–2266

www.rsc.org/njc

PAPER

Synthesis and physico-chemical characterization of bolaamphiphiles derived from alkenyl D-xylosides†‡

Magali Deleu,§[a] Céline Damez,§[b] Sylvain Gatard,[b] Katherine Nott,[a] Michel Paquot[a] and Sandrine Bouquillon*[b]

Received (in Montpellier, France) 24th February 2011, Accepted 7th June 2011
DOI: 10.1039/c1nj20158a

The two step synthesis of a new series of bolaamphiphiles derived from alkenyl D-xylosides is described. Yields between 57 and 90% have been reached. Aggregation behavior and membrane interaction properties of a particular sugar-bolaform composed of two xylose heads connected by an ether link to a hydrophobic chain comprising 18 carbon atoms and an insaturation were studied. Its CAC value (~0.05 mM) is low compared to those of conventional surfactants. Thermodynamic analysis has revealed that the aggregation phenomenon is mainly driven by an entropy process. The compound is able to interact with DPPC monolayers, in particular if their surface pressure is ≥ 15 mN m^{-1}. Our results highlight the potential of this bolaamphiphile as surfactant and membrane interacting agent.

Introduction

Sugar-based surfactants are compounds of interest for food, cosmetic and pharmaceutical applications because of their natural origin, their high biodegradability and their biocompatibility.

Our previous studies have shown the possibility of synthesizing pentosides having an octadienyl chain, with a double bond at the terminal position, from the Pd-catalyzed telomerisation of butadiene with pentoses.[1] 1-*O*-Alkenoyl-D-xylose and alkenyl D-xylosides were shown to exhibit interesting surface active properties.[2]

For many years, bolaform-type surfactants have received increasing attention because of their original properties. Their general structure consists of two polar heads connected by a hydrophobic spacer. In an aqueous environment, they have been reported to organize into aggregates of various morphologies depending on the nature of the polar head, and the length and flexibility of the spacer.[3] Potential applications of these compounds as encapsulation or vectorization agents have been reported.[4] Among bolaamphiphiles, sugar-based ones offer the advantages of providing the required hydrosolubility to the aggregates and reducing cytotoxicity.[5]

To our knowledge, the synthesis of sugar-based bolaforms mainly involves hexoses or disaccharides.[7–15] Pentose-based bolaforms have received less attention. Different symmetric sugar-based bolaamphiphiles have been synthesized. Their monosaccharidic glycosylated heads have a linear form[7] or a pyranose/furanose shape[4d,8–10] and are connected by ether bonds,[11] amide bonds[7,8] or acetalic functions[9e] to a hydrophobic spacer having a variable length. This lipophilic spacer can also be a simple or a double hydrocarbon chain.[4d,10,12]

Few dissymmetric bolaforms containing a sugar based head have been described in the literature. Gouéth *et al.*[9b] as well as Prata *et al.*[13] have prepared dissymmetric bolaamphiphilic compounds comprising two distinct saccharidic moieties. Other studies have described the synthesis of bolaforms with a sugar head and acidic,[14] or ammonium[15] hydrophilic heads. Other sugar-based bolaforms with two chains have also been prepared.[3b,c,4,6]

Sugar bolaamphiphiles have been reported to form ultrathin monolayer membranes and to be able to insert into lipid membranes.[12] Mixture of some bolaforms with conventional lipids leads to membranes with a higher stability against chemical and thermal degradation.[16a] In contrast, some monomeric and polymeric bolaamphiphiles can disrupt membranes.[16b]

In this paper, we first describe the synthesis of xylose-based bolaform surfactants. The novel symmetric bolaforms comprise two xylose polar heads connected by an ether or an ester link to a hydrocarbon segment with an insaturation and increasing chain lengths. In the second part, the aggregation behavior and the membrane interaction properties of a sugar-bolaform (**2′αα**) composed by two xylose heads connected by an ether link to a hydrophobic chain comprising 18 carbon atoms and an insaturation are investigated.

[a] *Unité de Chimie biologie industrielle, Gembloux Agro-Bio Tech, Université de Liège, 2, Passage des Déportés, B-5030 Gembloux, Belgium*
[b] *Unité Mixte de Recherche "Réactions Sélectives et Applications", CNRS - Université de Reims Champagne-Ardenne, Boîte n° 44, B.P. 1039, F-51687 Reims, France. E-mail: sandrine.bouquillon@univ-reims.fr; Fax: +33 (0) 3-26-91-31-66; Tel: +33 (0) 3-26-91-89-73*

† Dedicated to Prof. Didier Astruc on the occasion of his 65th birthday.
‡ Electronic supplementary information (ESI) available. See DOI: 10.1039/c1nj20158a
§ These authors have equally contributed to this work.

Results and discussion

Synthesis

The metathesis of acetylated xylosides having an octadienyl chain[1] was performed in the presence of Grubbs I catalyst to obtain six precursors of anomeric pure bolaform surfactants, **1**αα, **2**αα, **3**αα and **1**ββ, **2**ββ, **3**ββ with a spacer comprising, respectively, 10, 18 and 20 carbon atoms (Scheme 1). The synthesis isolated yields were comprised between 57 and 90%.

Metathesis reactions were undertaken under classical conditions in dichloromethane at 40 °C for 24 h. The precursor of bolaform **1**ββ resulting from the metathesis of hex-5′-enyl(2,3,4-tri-*O*-acetyl)-β-D-xylopyranoside was isolated with a yield of 74% with a single addition of the catalyst. Optimization of the metathesis reaction was carried out on the **1**αα compound by varying the mode of addition of the catalyst and its concentration. The compound **1**αα resulting from the metathesis of hex-5′-enyl(2,3,4-tri-*O*-acetyl)-α-D-xylopyranoside was obtained with a yield of 90% and of 87% by adding the catalyst in one shot or by two successive additions of catalyst respectively (Table 1, entries 3 and 2). These conditions were adopted for the synthesis of **2**ββ, **3**ββ and **3**αα and the yields obtained vary from 69% to 80%. For the preparation of compound **2**αα only, the catalyst was added 3 times with a metathesis yield reaching 69%. The αα and ββ derivatives react in a relatively similar way. However the metathesis is not stereoselective for the configuration of the double bond because both *Z* and *E* isomers are obtained and are not separable by chromatography on silica gel. NMR analysis showed that isomer *E* was by far the most abundant in all instances and was used to determine the ratio *Z*/*E*.

The acetylated precursors of the ether bolaforms were then deprotected in an almost quantitative way in the presence of sodium methanolate to give the desired bolaforms (Scheme 2). All compounds were obtained with a NMR purity higher than 95% after extraction.

The metathesis was also carried out with an unprotected xyloside, the hex-5′-enyl-α-D-xylopyranoside, to check the possibility of directly obtaining the bolaform (Scheme 3). This allowed the isolation of 1′,10′-bis-dec-5′-enyl-α-D-xylopyranoside **1**′αα with a yield of 75%.

As 1-*O*-alkenoyl-D-xylose has been shown to have very interesting surface active properties,[2] the metathesis of undec-10′-enoyl(2,3,4-tri-*O*-acetyl)-β-D-xylopyranoside and undec-10′-enoyl(2,3,4-tri-*O*-benzyl)-D-xylopyranoside was also studied.

Table 1 Metathesis reactions on xylosides: η and *Z*/*E* isomers ratio depending on the catalyst addition conditions

Entry	Catalyst addition conditions	Xyloside	η (%)	*Z*/*E*[a]
1	Fast[b]	**1**ββ	74	22/78
2	Fast[c]	**1**αα	87	26/74
3	Slow[d]		90	25/75
4	Slow[d]	**2**ββ	69	19/81
5	Fast[e]	**2**αα	69	15/85
6	Slow[f]	**3**ββ	76	18/82
7	Slow[d]	**3**αα	80	16/84

[a] Determined by ^{1}H NMR. [b] Addition by means of a transfer cannula. [c] Addition by means of a syringe $t_{addition}$ = 2 × 40 s (t = 0 and t = 12 h). [d] Addition in one shot by means of a syringe $t_{addition}$ = 4 h (Flow (Q) = 0.7 mL h^{-1}). [e] Addition by means of a syringe $t_{addition}$ = 3 × 40 s (every 2 h). [f] Addition by means of a syringe $t_{addition}$ = 2 h (Q = 0.7 mL h^{-1}).

The metathesis of undec-10′-enoyl(2,3,4-tri-*O*-acetyl)-β-D-xylopyranoside was performed in the presence of Grubbs I catalyst in dichloromethane (Scheme 4). The 1′,20′-bis-eicos-10′-enedioyl(2,3,4-tri-*O*-acetyl)-β-D-xylopyranoside **4**ββ was isolated with 67% yield.

For the deprotection, a mixture of triethylamine/methanol/water (1 : 8 : 1) known to selectively deprotect the acetylated ester derivatives of hexoses[17] was applied to compound **4**ββ (Scheme 5). In these conditions a mixture of free D-xylose and eicos-10-enedioate was obtained but not the expected bolaform.

Protection of the xylose hydroxyl groups by benzylic groups was then considered. Since no optimal conditions have been found to separate the α and β anomers of undec-10′-enoyl(2,3,4-tri-*O*-benzyl)-D-xylopyranoside by chromatography on silica gel, the metathesis was carried out on the mixture of anomers (Scheme 6, Table 2).

A single addition of the catalyst results in a yield not exceeding 46% (Table 2, entries 1 and 2). On the other hand, multiple additions of the catalyst yield 81% of 1′,20′-bis-eicos-10′-enedioyl(2,3,4-tri-*O*-benzyl)-D-xylopyranoside **5** (Table 2, entries 3 and 4).

To obtain the corresponding ester bolaform, the benzylic groups were hydrogenated. The different conditions employed are described in Scheme 7 and in Table 3.

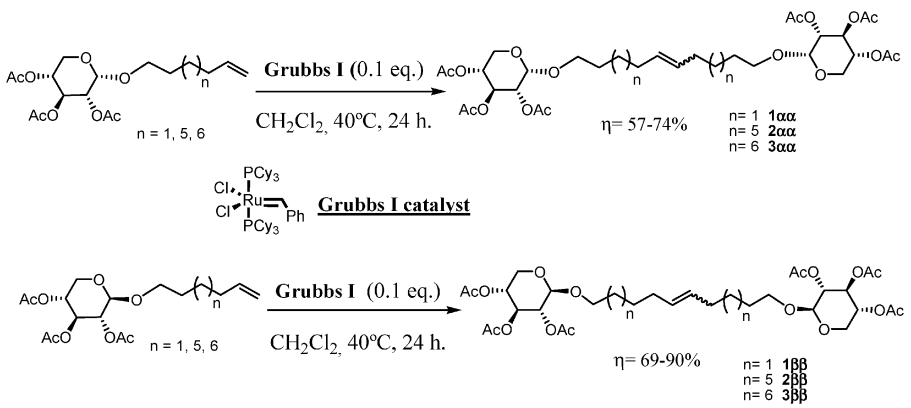

Scheme 1 Homodimerization reactions of xylosides having an octadienyl chain.

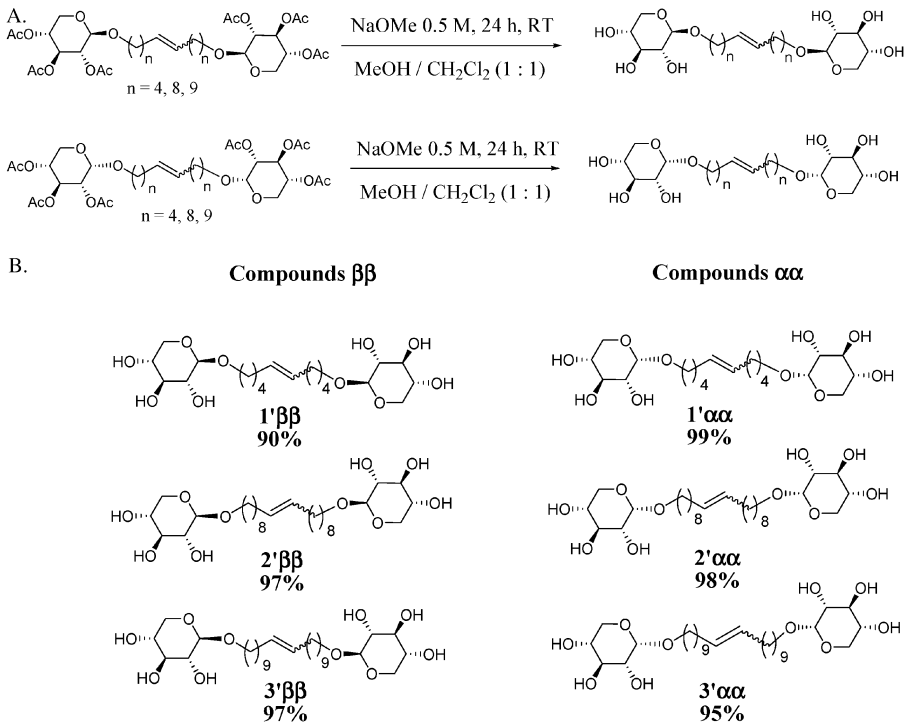

Scheme 2 A. Deprotection step of acetylated precursors of the bolaforms. B. Structure of the ether bolaform synthesized. The percentage indicated below each structure corresponds to the yields after isolation.

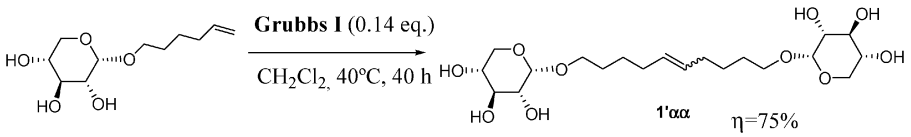

Scheme 3 Metathesis from hex-5′-enyl-α-D-xylopyranoside.

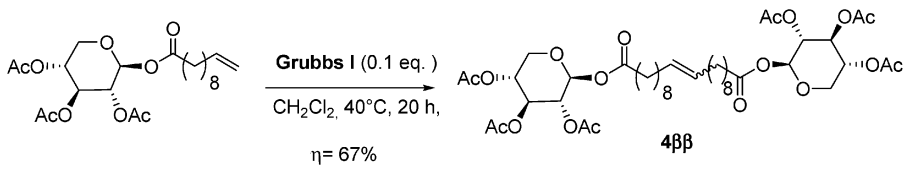

Scheme 4 Metathesis on undec-10′-enoyl(2,3,4-tri-*O*-acetyl)-β-D-xylopyranoside.

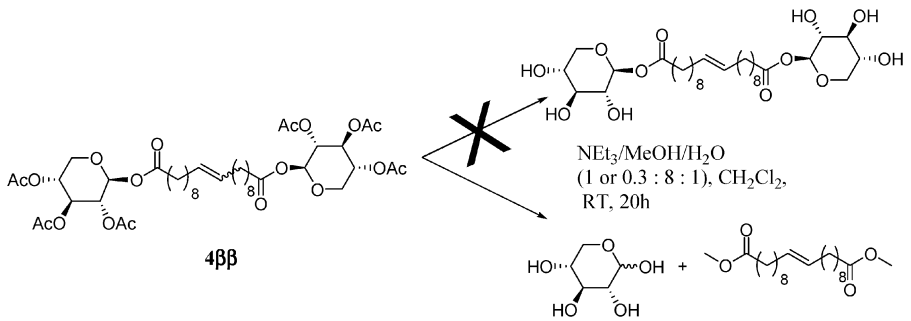

Scheme 5 Deprotection reaction of 1′,20′-bis-eicos-10′-enedioyl(2,3,4-tri-*O*-acetyl)-β-D-xylopyranoside **4**ββ.

Using Pd/C, 5 or 10%, no hydrogenation of the compound is observed (Table 3, entries 1–4). The deprotection of the benzylic groups takes place only when using $Pd(OH)_2/C$ (20%) in CH_2Cl_2/MeOH (1 : 20).[18] However, the mass spectrometry showed that 1′,20′-bis-eicosanedioyl-1-D-xylopyranoside was only obtained in the form of a mixture with partially

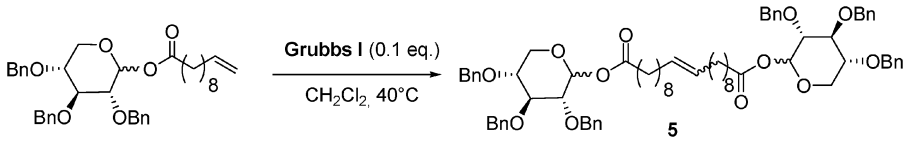

Scheme 6 Metathesis on undec-10′-enoyl(2,3,4-tri-*O*-benzyl)-D-xylopyranoside.

Table 2 Metathesis reactions on undec-10′-enoyl(2,3,4-tri-*O*-benzyl)-D-xylopyranoside[a]

Entry	Catalyst addition conditions	Reaction time/h	η (%)	E/Z[b]
1	Fast[c]	3	36	78/22
2	Fast[c]	14	46	
3	Fast[d]	24	72	
4	Fast[e]	51	81	

[a] Ester (100 mg, 017 mmol), Grubbs catalyst (14.1 mg, 0.017 mmol, 0.1 eq.) CH_2Cl_2 (7 mL), 40 °C. [b] Determined by ^{1}H NMR. [c] Addition by means of a transfer cannula. [d] Addition by means of a syringe $t_{addition}$ = 2 × 60 s (t = 0 and t = 12 h). [e] Addition by means of a syringe $t_{addition}$ = 2 × 60 s (t = 0, t = 9 h and t = 18 h).

Table 3 Hydrogenolysis reactions on 1′,20′-bis-eicos-10′-enedioyl-(2,3,4-tri-*O*-benzyl)-D-xylopyranoside[a]

Entry	Catalyst	Solvent	t/h	Conv. (%)
1	Pd/C (10%)	EtOH 99%	48	—
2	Janssen	EtOH/Et_2O (1/4)	72	—
3	Pd/C (5%)	EtOH 99%	48	—
4	Engelhart 5011	EtOH 95%	48	—
5	$Pd(OH)_2$/C (20%)	CH_2Cl_2/MeOH (1/20)	24	98%

[a] **5** (100 mg, 0.087 mmol), H_2 (1 atm.), RT.

deprotected compounds. Purification by chromatography on silica gel was fruitless.

Physico-chemical study

The potential of these sugar-based bolaforms as surfactants and membrane interacting agents has been studied by analysing the surface and the membrane interaction properties of the **2′αα** compound composed of two xylose heads connected by an ether link to a hydrophobic chain comprising 18 carbon atoms and an insaturation. Further examination of the relationships between the structure of these bolaamphiphiles and their physico-chemical properties will be performed in a future work. Indeed, the self-assembly properties of sugar-based bolaforms can be influenced by the stereochemistry of the glycosidic linkage and the length and the nature of the hydrocarbon chain (insaturated or not).[3c,19]

In the present study, the aggregation behaviour of **2′αα** in water was investigated by surface tension measurements and isothermal titration calorimetry (ITC). The mixing behaviour of **2′αα** with a dipalmitoylphosphatidylcholine (DPPC) monolayer taken as a simplified model membrane is analysed using surface pressure–area compression isotherms. Interaction of the bolaform with DPPC is also assessed by its ability to penetrate into a DPPC monolayer.

Aggregation behaviour. The aggregation behaviour of **2′αα** was first analysed by tensiometry measurements. The plot (Fig. 1) of the equilibrium surface tension as a function of **2′αα** concentration in the aqueous medium shows a break below 0.1 mM. As the solubility of **2′αα** in water is higher than 1 mM, the break indicates a saturation of the interface leading to a spontaneous formation of self-assemblies in the bulk. The intersection between the two linear fittings of the curve defines the critical aggregation concentration (CAC) and the corresponding surface tension (γ_{CAC}). At 25 °C, the CAC of **2′αα** is 0.052 mM and γ_{CAC} is ~44.0 mN m^{-1}. The dynamic light scattering measurement of a 100 μM solution of **2′αα** shows a single population at 227 ± 70 nm suggesting the presence of vesicles rather than micelles. However, symmetrical glucose bolaamphiphiles with a 12 or 14 carbon atoms hydrophobic chain have been shown to form helical crystalline nanofibers and no monolayer spherical vesicles.[19c] Further investigations using electron microscopy, small angle X-ray scattering and wide angle X-ray scattering[20] are necessary to determine the precise morphology of the **2′αα** supramolecular aggregates.

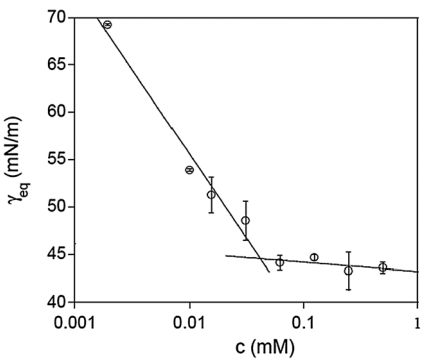

Fig. 1 Equilibrium surface tension (γ_{eq}) as a function of **2′αα** concentration (c) (logarithmic scale). Measurements were performed in milli-Q water at room temperature (25 ± 2 °C).

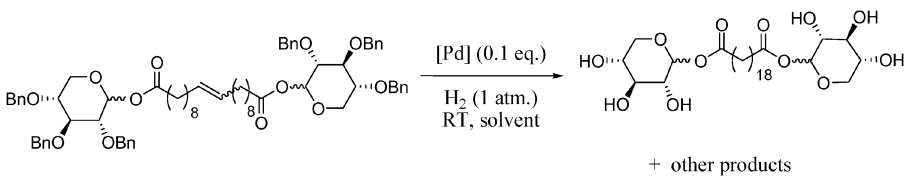

Scheme 7 Hydrogenation of 1′,20′-bis-eicos-10′-enedioyl(2,3,4-tri-*O*-benzyl)-D-xylopyranoside **5**.

In comparison with the critical micellar concentration (CMC) of conventional surfactants such as SDS, CTAB, CHAB, triton X-100[21] and alkyl glucoside,[22] **2′αα** CAC value is very low. It reflects its high capacity to aggregate. The absence of repulsive electrostatic forces between the neighbouring polar heads, as is the case for SDS and CTAB, favours such aggregation.

When the interface is saturated, the minimal area occupied by the molecule at the interface, a, can be determined by the equation:

$$a = 1/N_a\Gamma_m$$

where N_a is Avogadro's number and Γ_m is the maximal excess concentration of the surfactant at the surface calculated by the Gibbs equation:

$$\Gamma_m = -\frac{1}{2.303\,RT}\left(\frac{d\gamma}{d\log c}\right)$$

where R is the gas constant (8.314 J mol^{-1} K^{-1}), T is the absolute temperature and $d\gamma/d\log c$ is the slope of the curve of γ_{eq} as a function of the surfactant aqueous concentration ($\log c$) at concentrations below the CAC.

Under our conditions, the calculated a for **2′αα** is 81 Å^2. This value is almost twice the area occupied by an n-alkyl glycoside surfactant with one single glucose or mannose as polar head and a lipid chain between C8 and C12.[23] This suggests that bolaform molecules form a loop structure at the interface with both xylose heads close to each other and immersed in water as suggested for other bolaform types.[24] Unsurprisingly, a is lower than the one developed by hexose-based bolaforms at the air–water interface.[12] The configuration of the double bond of the spacer is not unique and ^{1}H NMR showed that the E isomer was by far the most abundant (Z/E ratio of 15/85). This should favor the extended shape of the spacer. However, according to the calculated a for **2′αα**, the presence of the insaturation in a long (18 carbon atoms) chain does not impair its flexibility, allowing it to adopt a bent conformation at the interface. Further investigations on xylose bolaamphiphiles with the corresponding saturated chain and/or with a shorter hydrophobic spacer could confirm this hypothesis. The geometry of the **2′αα** within the aggregate cannot be deduced from our results. In the case of vesicle formation, freeze fracture electron microscopy could be helpful for determining it.[15] Compression isotherms at an air–water interface of a Langmuir trough can also provide information about the conformation of bolaforms at an interface.[25]

Thermodynamic parameters associated with aggregate formation were determined by ITC. Injections of small volumes of a concentrated solution of **2′αα** into milli-Q water in the measurement cell are accompanied by an endothermic heat of reaction. After subtracting the heat related to the dilution of the drop, integration of each peak and normalization as a function of the number of surfactant moles injected, the molar heat of disaggregation ($\delta hi/\delta n$) is obtained. As the injections are performed, $\delta hi/\delta n$ decreases because the concentration of **2′αα** in the cell increases limiting the disaggregation phenomenon and finally reaches zero (Fig. 2). The inflection point

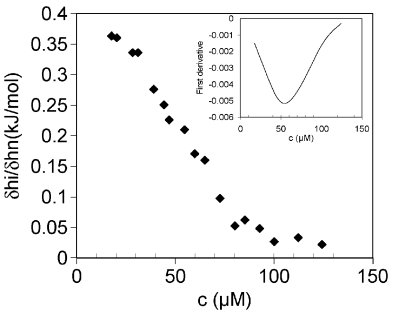

Fig. 2 Molar heat of **2′αα** disaggregation ($\delta hi/\delta n$) *versus* the concentration of **2′αα** (c) in the cell.

determined by the first derivative of $\delta hi/\delta n$ curve (see the inset) corresponds to the CAC. The value obtained is 0.053 mM and is in perfect accordance with the tensiometry measurements.

The step between the two plateaux of the sigmoid gives the enthalpy of disaggregation, equal in magnitude but opposite in sign to the aggregation enthalpy ($\Delta H^{w \rightarrow ag}$).[26] Under our experimental conditions, $\Delta H^{w \rightarrow ag}$ is −0.33 kJ mol^{-1}. The standard free energy of aggregate formation and the aggregation entropy can be calculated by the equation:

$$\Delta G^0_{ag} = RT\ln\left(\frac{CAC}{55.5}\right) = \Delta H - T\Delta S$$

where R, the gas constant, is 8.314 J mol^{-1} K^{-1}.

In our case, ΔG^0_{ag} is −34.1 kJ mol^{-1} and $T\Delta S$ is 33.8 kJ mol^{-1}.

At 25 °C, the aggregation of **2′αα** is spontaneous ($\Delta G < 0$), exothermic ($\Delta H < 0$) and generates a large positive change of the system entropy ($\Delta S > 0$) indicating a mainly entropy-driven process.

The large gain in entropy is caused by a reduction of the hydrophobic area that is exposed to water when aggregates are formed. The low contribution of the enthalpy to the Gibbs energy is not common for sugar-based surfactants for the temperature range used.[26] For octyl glucoside, changes in head group hydration between the monomeric and the micellar state of the surfactant have been assumed to add a constant enthalpic term. Our divergent result could be explained by a different hydration phenomenon of the xylose molecule (between the monomer and the aggregated state) comparatively to the glucose one, implying a distinct aggregation process. Indeed, the hydration of the sugar residue is known to influence the supramolecular arrangement of bolaamphiphiles[15] and according to Gray *et al.*[27] the aqueous solubility of xylose monomer is much higher than the glucose unit. Further investigations using spectroscopic methods,[28] for example, are necessary to elucidate this phenomenon.

Interaction with lipid monolayers. Compression isotherms of mixed **2′αα**–DPPC monolayers in different proportions were established in order to check the existence of interactions between these two compounds (Fig. 3).

At low molar ratios of bolaform ($0.10 \leq X_b \leq 0.50$), the isotherms of the mixed films lie between those of the pure components but they display a different overall shape. At $X_b = 0.25$ and 0.5, the characteristic transition observed in the DPPC isotherm is absent. Moreover, the maximal surface

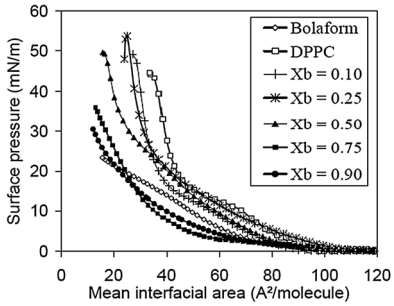

Fig. 3 Surface pressure–area isotherms of pure **2′**αα and DPPC monolayers and of mixed **2′**αα–DPPC monolayers at different bolaform molar ratios (X_b). The isotherms were recorded at 25 °C with milli-Q water as subphase. Duplicate experiments using separately prepared solutions gave similar results.

pressure is higher than the one reached with pure DPPC. These observations are in favour of the existence of interactions between the bolaform and DPPC molecules. In these proportions, these interactions have a stabilizing effect on the mixed monolayer, especially at high compression states. Compression isotherms of mixed films with a higher bolaform molar ratio (X_b = 0.75 and 0.90) are on the left hand side of the pure bolaform curve. Globally, molecules in these mixed films occupy a lower area than those of the pure compounds. It can arise from a particular arrangement of both molecules or from a destabilizing effect leading to a partial displacement of one or both compounds from the interface.

For two Π (10 and 20 mN m^{-1}), the plot of the molecular area *versus* X_b is shown in Fig. 4. The mixed monolayers X_b = 0.5 and 0.90 exhibit a molecular area significantly higher and lower, respectively, than those obeying the additivity rule (dashed line). According to Maget-Dana,[29] a deviation from the additivity rule means that specific interactions (*i.e.* excess interaction) exist between the two compounds. A positive deviation, such as observed at X_b = 0.5, suggests that one of the compound, at least, forms bidimensional aggregates at the interface as already observed for other surfactant/phospholipid mixed monolayers.[30] Negative deviation observed at X_b = 0.90 could result from formation of a complex between both molecules or from a partial displacement of the bolaform **2′**αα from the interface.

To further investigate the possible interactions between the bolaform molecules and DPPC, bolaform penetration into a

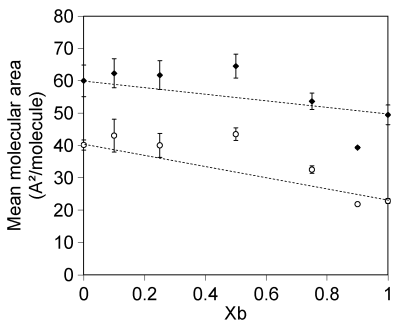

Fig. 4 Mean molecular area at a surface pressure of 10 (◆) and 20 (○) mN m^{-1} *versus* **2′**αα molar ratio of **2′**αα/DPPC mixtures (X_b). The dashed line represents the additivity rule values.

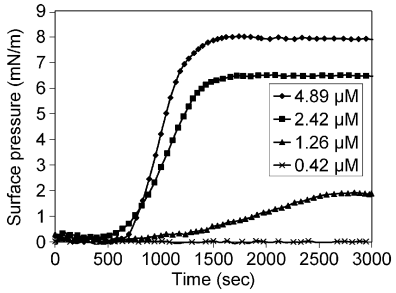

Fig. 5 Surface pressure increase as a function of the time elapsed after injection of increasing amounts of bolaform **2′**αα into the subphase (milli-Q water at 25 °C). The indicated concentrations are the final ones reached in the subphase.

DPPC monolayer was studied and results compared to the adsorption of the bolaform at a clean air–water interface.

Adsorption of **2′**αα at a clean interface (Fig. 5) is concentration dependent as is usually observed for conventional surfactants.[31] At 0.42 μM in the subphase, no effect on the surface pressure is observed. At higher concentrations, a significant increase of surface pressure is detected after a delay (~600 s) which is not influenced by the concentration of **2′**αα in the subphase. Nonetheless this concentration has an effect on the adsorption kinetics reflected by the slope of the linear part of the curve and on the maximal increase of surface pressure. The higher the concentration of bolaform in the subphase is, the steeper the slope is and the greater the equilibrium surface pressure is.

In the presence of a DPPC monolayer at the interface, the adsorption profile of the bolaform is modified (Fig. 6). For a DPPC monolayer initially compressed between 10 and 30 mN m^{-1}, the injection of bolaform molecules into the subphase (5 μM in the subphase) gives rise to a surface pressure increase giving evidence of bolaform penetration into the DPPC monolayer. The delay before surface pressure increase is shorter (100–250 s) than in the absence of DPPC. This suggests that DPPC molecules exert an attractive effect on the bolaform adsorption at the interface.

The maximal surface pressure increase depends on the initial surface pressure of the DPPC monolayer (Fig. 7).

At 15 mN m^{-1} and above, the variation is linear. Up to 31 mN m^{-1}, the increase is higher than in the absence of DPPC. According to Maget-Dana,[29] this means that specific interactions exist between the two compounds. The intersection

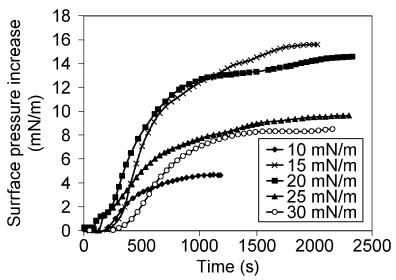

Fig. 6 Surface pressure increase as a function of the time elapsed after injection of bolaform **2′**αα (final concentration of 5 μM) into the subphase (milli-Q water at 25 °C) under a DPPC monolayer initially compressed at different surface pressures (between 10 and 30 mN m^{-1}).

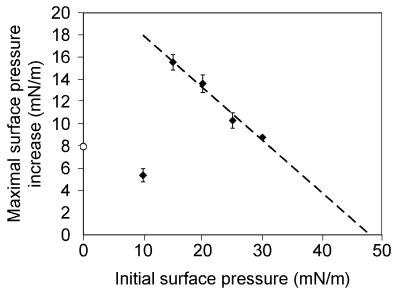

Fig. 7 Maximal surface pressure increase observed after the injection of bolaform **2′αα** as a function of the initial surface pressure of the DPPC monolayer. The white dot on the ordinate axis corresponds to the equilibrium surface pressure increase reached after adsorption of **2′αα** at a clean interface.

of the regression line with the *x*-axis determines the exclusion surface pressure (Π_{ex}), *i.e.* the maximal DPPC monolayer surface pressure permitting bolaform molecules penetration. Under our conditions, Π_{ex} is 48.6 mN m^{-1}. This is much higher than values observed for membrane active compounds such as mellitin, δ-lysin, paclitaxel and fengycin.[32] It suggests that bolaform **2′αα** is able to penetrate into biological membrane *in vivo*, for which Π is estimated to be between 31 and 34 mN m^{-1}.[33] Further investigation under more realistic conditions must be carried out to confirm this hypothesis.

Surprisingly, an initial surface pressure of 10 mN m^{-1} is unfavourable for bolaform insertion. The surface pressure increase is even lower than in the absence of DPPC. In other words, a lateral pressure threshold is necessary to allow bolaform to be inserted within the DPPC monolayer. To our knowledge, this biphasic aspect of the $\Delta\Pi$–Π_i plot has only been observed for charged peptides[29,34] for which electrostatic interactions play a crucial role in their interaction with the phospholipid layer. In our case, electrostatic forces cannot explain the results as the bolaform is uncharged. An optimal arrangement between **2′αα** and DPPC at a higher lateral pressure could be at the origin of the bolaform stabilization at the interface.

Conclusion

A novel series of bolaamphiphiles consisting of two xylose heads connected by an ester or an ether link to a hydrophobic spacer with increasing chain length and an insaturation were synthesized with satisfactory yields by sequential protection/metathesis/deprotection or by direct metathesis.

The interfacial behaviour and membrane interaction properties of the compound **2′αα** with a hydrophobic chain comprising 18 carbon atoms and connected by an ether link to both xylose heads with an α anomeric form were analyzed.

The important self-assembly properties of the xylose-based bolaform **2′αα** highlight its high potential as a surface-active agent. The aggregation is mainly driven by an entropy process. The area occupied by the molecule at the interface suggests that it adopts a loop structure. Its interaction with membrane lipids favours its adsorption and stabilization at the interface. This interaction occurs if the density of phospholipids is high enough to exert an optimal lateral pressure. Interaction of a hydrophobic nature between the aliphatic spacer of the bolaform and the hydrocarbon chains of phospholipids could lead to a stabilization of the bolaform molecules at the interface. Thanks to its membrane interaction properties, **2′αα** bolaform can be suggested as a potential component for the formulation of drug delivery systems.

Researches on the influence of the spacer length, of the insaturation and of the stereochemistry of the ether linkage of xylose-based bolaamphiphiles on their supramolecular organization and interaction properties with membrane models are in progress.

Experimental section

Syntheses

All reagents were commercially available and used as received. Solvents were dried and distilled under argon before use (CH_2Cl_2 over $CaCl_2$ and diethyl ether, THF over sodium/benzophenone) and stored over molecular sieves. ^1H and ^{13}C NMR spectra were recorded on an AC 250 Bruker in $CDCl_3$, MeOD or acetone-d_6 with TMS as reference for ^1H spectra and $CDCl_3$ (δ 77.0), MeOD (δ 49.9) or acetone-d_6 (δ 30.6) for ^{13}C spectra. The infrared spectra were recorded with Spectrafile IR™ Plus MIDAC. C, H and N analyses were performed on a Perkin Elmer 2400 CHN equipment. GC was recorded on a Hewlett-Packard HP-6890 gas chromatograph, fitted with DB-1 capillary column (25 m, 0.32 mm), a flame ionisation detector and HP-3395 integrator; chromatography was carried out on SDS Silica 60 (40–63 μm), Art 2050044 (flash-chromatography) or Silica 60 F_{254} (TLC plates).

All experiments (MS and HRMS) were obtained on a hybrid tandem quadrupole/time-of-flight (Q-TOF) instrument, equipped with a pneumatically assisted electrospray (Z-spray) ion source (Micromass, Manchester, UK) operated in positive mode. The electrospray potential was set to 3 kV in positive ion mode (flow of injection 5 μL min^{-1}) and the extraction cone voltage was usually varied between 30 and 90 V.

The detailed synthesis conditions for each compound are given in the ESI.‡

The purity of the compound **2′αα** was checked by RP-HPLC-ELSD (see below for the conditions) and was >97%.

Determination of 2′αα aqueous solubility

The **2′αα** concentrations in the aqueous medium were checked by external calibration by RP-HPLC-ELSD on an Agilent Technologies 1200 series HPLC. The column, a Zorbax XDB C18 (3.5 μm, 4.6 × 150 mm, Agilent), was thermostated at 30 °C. The flow rate was 0.8 mL min^{-1} and a linear gradient of milli-Q water and ACN starting at 30% ACN and increasing to 100% ACN in 5 min was used. Then, 100% ACN was maintained for 5 min. The ELSD parameters were 40 °C and 3.5 bars N_2.

Molecular aggregation in water

By tensiometry. Equilibrium surface tension was measured with the tensiometer Tensimat N3 (Prolabo) equipped with a platinum Wilhelmy plate at room temperature (25 ± 2 °C).

The bolaform **2′αα** was dissolved in dimethylsulfoxide (DMSO) and the concentrated organic solution was diluted with milli-Q water (final DMSO concentration of 1% (v/v)). All measurements were repeated twice with two distinct bolaform solutions.

By dynamic light scattering. Particle size distribution of a 100 μM **2′αα** aqueous dispersion was measured using a Delsa™ Nano (Beckman Coulter, Brea, CA, USA). The bolaform **2′αα** was dissolved in DMSO and the concentrated organic solution was diluted with milli-Q water (final DMSO concentration of 1% (v/v)).

By isothermal titration calorimetry. The thermodynamic parameters associated with the aggregation were determined by isothermal titration calorimetry performed on a VP-ITC Microcalorimeter (Microcal, Northampton USA).

Aliquots of 4 μL of a 1.2 mM bolaform **2′αα** solution were injected into the calorimeter cell (V_{cell} = 1.4565 mL) containing milli-Q water with 1% (v/v) of DMSO at constant time intervals (300 s). The cell was maintained very accurately at 25 °C.

The bolaform **2′αα** solutions in milli-Q water were prepared as for the experiments with the tensiometer.

The solution in the sample cell was stirred at a speed of 305 rpm. The reference cell was filled with milli-Q water. Prior to each analysis, all solutions were degassed using a sonicator bath.

The heats related to the fall of the drop were determined by injecting at constant time interval 4 μl of water with 1% (v/v) of DMSO into the measuring cell containing water with 1% (v/v) of DMSO. These values were subtracted from the observed heats for determining the effective heats. All measurements were repeated twice with two distinct bolaform solutions. Raw data were processed by software Origin 7 (Originlab, Northampton, USA).

Monolayer studies by the Langmuir trough technique

For compression isotherm experiments, bolaform **2′αα** and dipalmitoylphosphatidylcholine (DPPC) monolayers were studied at 25 ± 0.2 °C with an automated LB system (KSV minitrough, KSV Instruments Ltd., Helsinki, Finland).

Bolaform **2′αα** or DPPC were dissolved in dichloromethane/methanol (9 : 1 v/v) at 1.35 mM. Pure solutions as well as mixtures of bolaform **2′αα** and DPPC at different bolaform molar ratios (X_b = 0.1, 0.25, 0.5, 0.75 and 0.9) were spread on milli-Q water. After waiting for 15 min to allow for solvent evaporation and spreading of the molecules, the monolayers were compressed at a rate of 3 mm min^{-1}. The surface pressure of the monolayer was measured using a platinum Wilhelmy plate with an accuracy of 0.1 mN m^{-1}. The difference between the molecular areas of two independent sets of measurements was less than 10%.

For adsorption experiments, bolaform, solubilized in DMSO, was injected (20 μL) into the subphase (milli-Q water) to final concentrations of 4.89 × 10^{-6} M, 2.42 × 10^{-6} M, 1.26 × 10^{-6} M and 0.42 × 10^{-6} M. The injection was done using a Hamilton syringe and two homemade devices allowing the injection of bolaform without disturbing the air–water interface. These devices were placed at two fixed positions on the trough to ensure a reproducible injection process. Furthermore, during the entire duration of the experiment, the subphase was stirred using two cylindrical micromagnetic rods (8 × 1.5 mm^2) and two electronic stirrer heads located beneath the trough (model 300, Rank Brothers, Bottisham, U.K.). An autoreversing mode with slow acceleration and a stirring speed of 100 rpm was selected. After the injection of bolaform, the increase in surface pressure was recorded.

For the penetration experiments, DPPC monolayers were prepared with the same LB system as above. The defined initial surface pressure of these monolayers was obtained by spreading a precise volume of a DPPC 1 mM solution prepared in dichloromethane/methanol (9 : 1 v/v). As soon as the initial surface pressure was stabilized (~20 min), bolaform, solubilized in DMSO, was injected (20 μL) into the subphase (milli-Q water) to a final concentration of 5 × 10^{-6} M using the same injection setup as described above. After the injection of bolaform, the increase in surface pressure was recorded.

Pure DMSO injections into the subphase did not modify the initial surface pressure of the DPPC monolayers within the time span of the penetration experiments.

Acknowledgements

This work was supported by the "Contrat d'objectifs" in "Europol'Agro" framework (Glycoval program). We are grateful to the public authorities of Champagne-Ardenne for a fellowship to C. D. and material funds. The authors thank Julien Ertel and Alexandre Schandeler for their technical assistance. M. D. thanks the F.R.S.-F.N.R.S. (National Funds for Scientific Research, Belgium) for her research associate position. K. N. thanks the Superzym ARC grant, financed by the French Community of Belgium.

References

1 (*a*) J. Muzart, F. Hénin, B. Estrine and S. Bouquillon, *French Patent CNRS No.*, 0116363 *PCT WO* 03053987, 2001; (*b*) B. Estrine, S. Bouquillon, F. Hénin and J. Muzart, *Eur. J. Org. Chem.*, 2004, 2914; (*c*) B. Estrine, S. Bouquillon, F. Hénin and J. Muzart, *Green Chem.*, 2005, **7**, 219; (*d*) C. Hadad, C. Damez, S. Bouquillon, B. Estrine, F. Hénin, J. Muzart, I. Pezron and L. Komunjer, *Carbohydr. Res.*, 2006, **341**, 1938; (*e*) C. Damez, B. Estrine, A. Bessmertnykh, S. Bouquillon, F. Hénin and J. Muzart, *J. Mol. Catal. A: Chem.*, 2006, **244**, 93; (*f*) B. Estrine, S. Bouquillon, F. Hénin and J. Muzart, *Appl. Organomet. Chem.*, 2007, **21**, 945.

2 C. Damez, S. Bouquillon, D. Harakat, F. Hénin, J. Muzart, I. Pezron and L. Komunjer, *Carbohydr. Res.*, 2007, **342**, 154.

3 (*a*) S. Franceschi, V. Andreu, N. de Viguerie, M. Riviere, A. Lattes and A. Moisand, *New J. Chem.*, 1998, **22**, 225; (*b*) J. H. Fuhrhop and T. Wang, *Chem. Rev.*, 2004, **104**, 2901; (*c*) T. Benvegnu, M. Brard and D. Plusquellec, *Curr. Opin. Colloid Interface Sci.*, 2004, **8**, 469; (*d*) A. Polidori, M. Wathier, A.-M. Fabiano, B. Olivier and B. Pucci, *ARKIVOC*, 2006, **iv**, 73.

4 (*a*) J. H. Fuhrhop and J. Köning, in *Monographs in Supramolecular Chemistry no 5, Membranes and Molecular Assemblies, The Synkinetic Approach*, ed. J. Fraser Stoddart, The Royal Society of Chemistry, Cambridge, UK, 1994; (*b*) P. Bandyopadhyay and P. K. Bharadwaj, *Langmuir*, 1998, **14**, 7537; (*c*) P. Lo Nostro, G. Briganti and S. H. Chen, *J. Colloid Interface Sci.*, 1991, **142**, 214; (*d*) F. Brisset, R. Garelli-Calvet, J. Azema, C. Chebli, I. Rico-Lattes and A. Lattes, *New J. Chem.*, 1996, **20**, 595;

(*e*) I. Rico-Lattes and A. Lattes, *Colloids Surf., A*, 1997, **123–124**, 37.
5 S. Denoyelle, A. Polidori, M. Brunelle, P. Y. Vuillaume, S. Laurent, Y. ElAzhary and B. Pucci, *New J. Chem*., 2006, **30**, 629.
6 (*a*) J. H. Fuhrhop, M. Krull, A. Schulz and D. Möbius, *Langmuir*, 1990, **6**, 497; (*b*) I. Rico-Lattes, M. F. Gouzy, C. André-Barrès, B. Guidetti and A. Lattes, *New J. Chem*., 1998, **22**, 451; (*c*) J. H. Fuhrhop, D. Spiroski and C. Boettcher, *J. Am. Chem. Soc*., 1993, **115**, 1600.
7 R. Garelli-Clavet, F. Brisset, I. Rico and A. Lattes, *Synth. Commun*., 1993, **23**, 35.
8 (*a*) M. Masuda and T. Shimizu, *Chem. Commun*., 1996, 1057; (*b*) T. Shimizu and M. Masuda, *J. Am. Chem. Soc*., 1997, **119**, 2812; (*c*) M. Masuda and T. Shimizu, *J. Carbohydr. Chem*., 1998, **17**, 405–416; (*d*) M. Masuda, V. Vill and T. Shimizu, *J. Am. Chem. Soc*., 2000, **122**, 12327.
9 (*a*) J. H. Fuhrhop, H. H. David, J. Mathieu, U. Liman, H. J. Winter and E. Boekema, *J. Am. Chem. Soc*., 1986, **108**, 1785; (*b*) P. Gouéth, A. Ramiz, G. Ronco, G. Mackenzie and P. Villa, *Carbohydr. Res*., 1995, **266**, 171; (*c*) H. Ramza, G. Descotes, J. M. Basset and A. Mutch, *J. Carbohydr. Chem*., 1996, **15**, 125; (*d*) D. Lafont, P. Boulanger and Y. Chevalier, *J. Carbohydr. Chem*., 1995, **14**, 533; (*e*) S. C. Ats, J. Lehman and S. Petry, *Carbohydr. Res*., 1994, **252**, 325; (*f*) R. Dominique, S. K. Das and R. Roy, *Chem. Commun*., 1998, 2437–2438; (*g*) M. Tsuzuki and T. Tsuchiya, *Carbohydr. Res*., 1998, **311**, 11.
10 J. N. Bertho, A. Coué, D. F. Ewing, J. W. Goodby, P. Letellier, G. Mackenzie and D. Plusquellec, *Carbohydr. Res*., 1997, **300**, 341.
11 L. Clary, C. Gadras, J. Greiner, J. P. Rolland, C. Santaella, P. Vierlingn and A. Gulik, *Chem. Phys. Lipids*, 1999, **99**, 125.
12 C. Satgé, R. Granet, B. Verneuil, Y. Champavier and P. Krausz, *Carbohydr. Res*., 2004, **339**, 1243.
13 C. Prata, N. Mora, A. Polidori, J. M. Lacombe and B. Pucci, *Carbohydr. Res*., 1999, **321**, 15.
14 J. Sirieix, N. Lauth de Viguerie, M. Rivière and A. Lattes, *New J. Chem*., 2000, **24**, 1043.
15 J. Guilbot, T. Benvegnu, N. Legros, D. Plusquellec, J. C. Dedieu and A. Gullik, *Langmuir*, 2001, **17**, 613.
16 (*a*) G. Mao, Y.-H. Tsao, M. Tirrell and H. T. Davis, *Langmuir*, 1994, **10**, 4174; (*b*) G. Escamilla and G. Newkome, *Angew. Chem., Int. Ed. Engl*., 1994, **33**, 1937.
17 (*a*) A. Lubineau, E. Meyer and P. Place, *Carbohydr. Res*., 1992, **228**, 191; (*b*) C. Bliard, G. Massiot and S. Nazabadioko, *Tetrahedron Lett*., 1994, **35**, 6107.
18 K. Yoshida, S. Nakajima, T. Wakamatsu, Y. Ban and M. Shibasaki, *Heterocycles*, 1988, **27**, 1167.
19 (*a*) R. Auzély-Velty, T. Benvegnu, G. Mackenzie, J. A. Haley, J. W. Goodby and D. Plusquellec, *Carbohydr. Res*., 1998, **314**, 65; (*b*) G. Lecollinet, A. Gulik, G. Mackenzie, J. W. Goodby, T. Benvegnu and D. Plusquellec, *Chem.–Eur. J*., 2002, **8**, 585; (*c*) T. Benvegnu, G. Lecollinet, J. Guilbot, M. Roussel, M. Brard and D. Plusquellec, *Polym. Int*., 2003, **52**, 500.
20 M. Berchel, C. Mériadec, L. Lemiègre, F. Artzner, J. Jeftié and T. Benvegnu, *J. Phys. Chem. B*, 2009, **113**, 15433.
21 (*a*) T. Rabilloud, S. Fath, E. vom Baur, J.-M. Egly and O. Revelant, *Le technoscope de Biofutur*, 1993, **126**, 1; (*b*) P. Mukerjee and K. J. Mysels, *National standard reference data series No. 36*, U.S. National Bureau of Standards, Washington, DC; (*c*) S. Dai and K. C. Tam, *Colloids Surf., A*, 2003, **229**, 157.
22 (*a*) M. R. Wenk and J. Seelig, *J. Phys. Chem*., 1997, **101**, 5224; (*b*) H. Heerklotz and J. Seelig, *Biophys. J*., 2000, **78**, 2435.
23 S. Matsumara, K. Imai, S. Yoshikawa, K. Kawada and T. Uchibori, *J. Am. Oil Chem. Soc*., 1990, **67**, 996.
24 K. Kohler, A. Meister, B. Dobner, S. Drescher, F. Ziethe and A. Blume, *Langmuir*, 2006, **22**, 2668.
25 A. Jacquemet, V. Vié, L. Lemiègre, J. Barbeau and T. Benvegnu, *Chem. Phys. Lipids*, 2010, **163**, 794.
26 S. Paula, W. Süs, J. Tuchtenhagen and A. Blume, *J. Phys. Chem*., 1995, **99**, 11742.
27 M. C. Gray, A. O. Converse and C. E. Wyman, *Appl. Biochem. Biotechnol*., 2003, **105–108**, 179.
28 B. Lindman, H. Wennerström, H. Gustavsson, N. Kamenka and B. Brun, *Pure Appl. Chem*., 1980, **52**, 1307.
29 R. Maget-Dana, *Biochim. Biophys. Acta, Biomembr*., 1999, **1462**, 109.
30 (*a*) M. Deleu, H. Razafindralambo, Y. Popineau, P. Jacques, P. Thonart and M. Paquot, *Colloids Surf., A*, 1999, **152**, 3; (*b*) M. Eeman, M. Deleu, M. Paquot, P. Thonart and Y. Dufrene, *Langmuir*, 2005, **21**, 2505.
31 (*a*) G. Geeraerts, P. Joos and F. Ville, *Colloids Surf., A*, 1995, **95**, 281; (*b*) V. B. Fainerman, A. V. Makievski and R. Miller, *Colloids Surf., A*, 1994, **87**, 61.
32 (*a*) M. Bhakoo, T. H. Birbeck and J. H. Freer, *Biochemistry*, 1982, **21**, 6879; (*b*) A. Preetha, N. Huilgol and R. Banerjee, *Colloids Surf., B*, 2006, **53**, 179; (*c*) M. Deleu, M. Paquot and T. Nylander, *Biophys. J*., 2008, **94**, 2667.
33 D. Marsh, *Biochim. Biophys. Acta*, 1996, **1286**, 183.
34 R. Maget-Dana and M. Ptak, *Biophys. J*., 1995, **68**, 1937.

